

Modulation of NLRP3 Inflammasome Activation by QYHT Decoction: Implications for the Treatment of Erectile Dysfunction in Hyperuricemia

American Journal of Men's Health
January-February 1–20
© The Author(s) 2025
Article reuse guidelines:
sagepub.com/journals-permissions
DOI: 10.1177/15579883251318307
journals.sagepub.com/home/jmh



Pingyu Ge¹, Yinxue Guo¹, Bangwei Che², Hang Jin¹, Lan Chen¹, Zhichao Chen¹, and Kaifa Tang² 

Abstract

Hyperuricemia (HUA) causes vascular endothelial dysfunction and oxidative stress, and simultaneously activates the NLRP3 inflammasome, leading to inflammatory reactions and erectile dysfunction (ED). This study aimed to investigate the effects of QYHT (Quyuhuanerxian decoction) decoction on the NLRP3 inflammasome and explore its potential in treating HUA-induced ED. This study employed four treatment methods: (a) treating HUA-induced ED patients with QYHT and analyzing changes in gut microbiota abundance and fecal metabolites through 16S sequencing; (b) establishing an HUA-induced ED rat model, treating with different doses of QYHT, and examining changes in serum metabolites; (c) conducting fecal microbiota transplantation (FMT) therapy; evaluating erectile function, oxidative stress, inflammatory response, and NLRP3 inflammasome activation levels; and (d) exploring key monomeric compounds and potential targets in QYHT through network pharmacology and molecular docking. The treatment with QYHT and FMT increased testosterone levels, reduced oxidative stress and inflammatory marker levels, and inhibited the expressions of NLRP3-related factors. QYHT affected the gut microbiota structure and metabolite levels. The key components were linoleoyl acetate and mandanol, and the target was JAK2. QYHT decoction regulates the distribution of gut microbiota, improves amino acid metabolism, and effectively inhibits the activation of NLRP3 inflammasomes. This, in turn, enhances erectile function and reduces oxidative stress and inflammatory response levels, leading to successful treatment of HUA-induced ED.

Keywords

hyperuricemia, inflammatory reactions, erectile dysfunction, QYHT decoction

Received December 9, 2024; revised January 13, 2025; accepted January 18, 2025

Introduction

An increase in the production or decrease in the excretion of uric acid leads to elevated serum uric acid levels. Hyperuricemia (HUA) is a condition in which the concentration of uric acid in the blood is higher than the normal range. The prevalence of HUA varies significantly across the regions. For example, in the United States, the overall prevalence of HUA is 21% (21.2% in males and 21.6% in females) (Zhu et al., 2011), while in Japan, it is 25.8% (34.5% in males and 11.6% in females) (Nagahama et al., 2004), and in mainland China, it is 13.3% (19.4% in males and

7.9% in females) (R. Liu et al., 2015). Within the normal range, uric acid exhibits anti-inflammatory, antioxidant, and vasodilatory effects (Becker et al., 1991).

¹First Clinical College of Guizhou University of Traditional Chinese Medicine, Guiyang, China

²Department of Urology Surgery, First Affiliated Hospital of Guizhou University of Traditional Chinese Medicine, Guiyang, China

Corresponding Author:

Kaifa Tang, Department of Urology Surgery, First Affiliated Hospital of Guizhou University of Traditional Chinese Medicine, No. 71 Baoshan North Road, Guiyang, Guizhou 550001, China.
Email: kaifatang@finmail.com



Creative Commons Non Commercial CC BY-NC: This article is distributed under the terms of the Creative Commons Attribution-NonCommercial 4.0 License (<https://creativecommons.org/licenses/by-nc/4.0/>) which permits non-commercial use, reproduction and distribution of the work without further permission provided the original work is attributed as specified on the SAGE and Open Access pages (<https://us.sagepub.com/en-us/nam/open-access-at-sage>).

However, elevated blood uric acid levels can lead to metabolic disorders and various diseases (W. C. Liu et al., 2012). Erectile dysfunction (ED) is defined as the inability to achieve or maintain sufficient erection of the penis for satisfactory sexual activity during the past 3 months. The prevalence of ED was 5.1% in males aged 29 to 30, 14.8% in males aged 40 to 59, and 44% in males aged 60 to 69 (Calzo et al., 2021). More than 50% of males aged 70 years and above are diagnosed with ED (Shamloul & Ghanem, 2013). The primary pathogenesis of ED is endothelial dysfunction and atherosclerosis (Ibrahim et al., 2018; Koroglu et al., 2018).

HUA level is an independent risk factor for ED (Long et al., 2016). The main reasons for HUA-induced ED are as follows: (a) HUA directly inhibits the relaxation function of penile corpus cavernosum smooth muscles, disrupting the dynamic balance between endothelium-derived relaxing factor (EDRF) and endothelin (ET) in the blood vessels, leading to dysfunction in the contraction function of penile corpus cavernosum vascular smooth muscle cells; (b) HUA upregulates the activity of RhoA/Rho kinase, resulting in enhanced contraction of penile vascular smooth muscles and consequently causing stasis in the corpus cavernosum (Rajasekaran et al., 2005); and (c) HUA stimulates the production of inflammatory mediators, causing damage to the vascular endothelium and promoting abnormal vascular endothelial function. There is a close association between uric acid and NLR family pyrin domain-containing 3 (NLRP3) inflammasomes. NLRP3 inflammasomes are multi-protein complexes composed of NLRP3, apoptosis-associated speck-like protein-containing CARD (ASC), and caspase-1. As an intracellular pattern recognition receptor, NLRP3 can be activated by HUA or uric acid crystals, promoting the secretion of interleukin (IL)-1 β , IL-18 β , and IL-18, which leads to the development of various inflammatory diseases (Martinon et al., 2006; Vilaysane et al., 2010; Wen et al., 2021). NLRP3 can activate endothelin-1-induced ED (Sobrano Fais et al., 2023). Similarly, NLRP3 regulation can improve experimental HUA (Sun et al., 2021) or hyperuricemic nephropathy (Wen et al., 2021). In addition, studies have shown that inhibition of NLRP3 can alleviate chronic renal dysfunction caused by HUA (Cui et al., 2020).

Traditional Chinese medicine believes that the occurrence of ED is rooted in damage to the liver, kidneys, heart, and spleen, leading to deficiency of qi and blood and blockage of the meridians. Consequently, this results in malnourishment of the penile tendons, leading to impotence. The prescription of Erxian

Decoction comes from the "Obstetrics and Gynecology." The decoction has the effects of warming kidney yang, replenishing kidney essence, purging kidney fire, and regulating Chong and Ren meridians. It is widely used in the treatment of diseases such as kidney yin and kidney yang deficiency. Erxian Decoction was used to treat various symptoms of women before and after menopause (Wang et al., 2019). However, there are few reports on its efficacy in male ED. In response to this issue, researchers improved Erxian Decoction and developed QYHT Decoction, comprising semen coicis, semen plantaginis, thunberg fritillary bulb, earthworm, herba epimedii, and rhizoma curculiginis. This decoction is capable of resolving phlegm and dispersing stasis, effectively alleviating the obstruction caused by phlegm dampness, promoting smooth blood circulation, reducing the impact on vital organs, such as the kidneys, and thereby lowering the occurrence of related complications, including ED. Our previous research found that QYHT combined with febuxostat can improve penile hemodynamics, endothelial function, and ED in patients with HUA (Ge et al., 2018; Ge & Guo, 2020). Subsequently, we found in our study on rats that QYHT may reduce the damage of vascular endothelial function in the corpus cavernosum of ED rats with high uric acid blood by inhibiting the inflammatory response mediated by NLRP3 inflammasome in the corpus cavernosum tissue and improving erectile function (Xie et al., 2023).

Therefore, this study aimed to investigate the therapeutic effects and mechanisms of QYHT decoction on ED induced by HUA.

Method

Recruitment of Participants and Sample Collection

A total of 30 subjects were included in this study, who were randomly divided into three groups including the control ($n = 10$), HUA-induced ED ($n = 10$), and QYHT decoction treatment ($n = 10$) groups. The control group consisted of healthy individuals who underwent physical examinations at our hospital during the same period. The specific procedure for the QYHT decoction treatment group was as follows. A mixture of 20 g of semen coicis, 10 g of semen plantaginis, 20 g of thunberg fritillary bulb, 20 g of earthworm, 10 g of herba epimedii, and 10 g of rhizoma curculiginis was prepared by boiling with water and filtered to yield 300 mL of decoction. Patients took 100 mL of the decoction orally half an hour after meals, three times a day, for a continuous treatment period of 12 weeks. At the end of the treatment, whole blood, serum, and

stool samples would be collected from each subject in each group.

The inclusion criteria were as follows: meeting the diagnostic criteria for HUA (uric acid level >420 $\mu\text{mol/L}$); International Index of Erectile Function-5 (IIEF-5) score between 8 and 21; married males, aged <55 years, with regular sexual activity and a stable sexual partner; ED occurring after the onset of HUA; normal genital and secondary sexual characteristics; no history of ED medication use in the past 3 months; exclusion of psychogenic ED through detailed medical history, comprehensive physical examination, and endocrine testing; and no history of trauma or surgery in the past 6 months. The exclusion criteria were as follows: the use of diuretics or other medications affecting uric acid levels within 1 week before diagnosis, abnormal liver or kidney function, the presence of other sexual dysfunction, acute or chronic inflammation of the reproductive system, history of long-term heavy alcohol consumption, and the presence of mental abnormalities.

Establishment of HUA-Induced ED Rat Model

We conducted experiments using 60 male SD rats aged 6 to 8 weeks. The rats were randomly divided into five groups: a control group, a model group, and low, medium, and high-dose groups ($n = 12$ per group). The model group and the low, medium, and high-dose groups were fed with feed containing yeast powder (15 g/kg), administered ethyl carbamate suspension (250 mg/kg) by gavage, and injected subcutaneously with potassium oxonate (200 mg/kg) to induce the model. The control group was fed regular feed and treated with an equivalent volume of physiological saline. The modeling period lasted for 8 weeks. On the 57th day, blood was collected from the rat tail vein, centrifuged at 4,000 r/min for 15 min to obtain serum. The levels of UA, blood urea nitrogen (BUN), and Cr were measured using an AMS-18 automatic analyzer to verify the successful establishment of the HUA model. Subsequently, HUA-induced ED rats were identified. Rats were placed in an observation cage under dim light, allowed to adapt to the environment for 10 min, and then subcutaneously injected with apomorphine (APO, 100 $\mu\text{g/kg}$) and observed for 30 min. Rats showing penile erection were classified as APO (+) HUA rats, while those without penile erection were classified as HUA-induced ED rats. The screened HUA-induced ED rats were administered QYHT decoction by gastric lavage. Based on human clinical doses, the rats were given low, medium, and high

doses of QYHT decoction at 9.45, 18.9, and 37.8 mg/kg, respectively, once daily for 28 days.

Complete Blood Count and Blood Biochemical Index Detection

Whole blood from the collected subjects underwent complete blood count analysis using a DxH 900 hematology analyzer (Beckman, USA). In addition, blood biochemical parameters were measured using an Atellica automatic biochemical analyzer (Siemens, Germany).

Network Pharmacology Analysis

We employed the Traditional Chinese Medicine Systems Pharmacology (TCMSP) database and analysis platform to procure the primary constituents of the QYHT decoction from various medicinal herbs. Subsequently, a rigorous selection process was undertaken, focusing on components with a bioavailability of 30% or higher and a drug-likeness value ≥ 0.18 or above. Using the SwissTargetPrediction and Pharmapper databases, we cross-referenced the target points of active ingredients with Genecards to identify gene targets relevant to the associated disease. Through an intersectional analysis between the target points of the active ingredients and those related to the disease, the identified common targets were deemed as potential focal points for the QYHT decoction in the treatment of HUA-induced ED.

Molecular Docking

The 3D configuration was obtained from the TCMSP database (<https://tcmspw.com/tcmsp.php>), and the molecular structures were obtained from the PDB database (<https://www.rcsb.org/>). By employing PYMOL 2.3.4, we subjected the target proteins to dehydration and deliganding. Subsequently, AutoDock 4.2.6 software was utilized for the hydrogenation of target proteins and computation of charge, with parameters for the duly configured docking grid. Molecular docking was carried out with the AutoDock Vina 1.1.2 program, based on the binding affinity calculated by the scoring function, the top 10 conformational models with the highest scores were screened out, and the conformational docking with the smallest binding energy was selected.

Serum ELISA

The levels of nitric oxide (NO), testosterone (T), malondialdehyde (MDA), C-reactive protein (CRP),

Table 1. The Primer Sequences Employed in the qPCR Experiment

Primer	Sequences
h-NLRP3-F	CCGTCGTCTTTGAGCCTTCT
h-NLRP3-R	GGATGGATCGCAGCTCTCTC
h-ASC-F	ATCCAGGCCCTCCTCAG
h-ASC-R	AGAGCTTCCGCATCTTGCTT
h-caspase-1-F	GTGCAGGACAACCCAGCTAT
h-caspase-1-R	CGTGCTGTCAGAGGTCTTGT
h-GAPDH-F	TCAAGGCTGAGAACGGGAAG
h-GAPDH-R	TCGCCCCACTTGATTTTGA
r-NLRP3-F	CTGTGTGGATCTTTGCAGCG
r-NLRP3-R	CAAATCGAGATGCGGGAGAGA
r-ASC-F	TGCTGGATGCTCTGTATGGC
r-ASC-R	GTCACCAAGTAGGGCTGTGT
r-caspase-1-F	GACCGAGTGTTCCCTCAAG
r-caspase-1-R	GACGTGTACGAGTGGGTGTT
r-GAPDH-F	CAATCCTGGGCGGTACAAC
r-GAPDH-R	TACGGCCAAATCCGTTTACA

tumor necrosis factor- α (TNF- α), estradiol (E2), and endothelin-1 (ET-1) in the serum were referenced according to the instructions of the respective assay kits from mlbio for NO and from RayBiotech for T, MDA, CRP, and TNF- α .

qPCR

Blood RNA extraction was performed according to the PureLink Total RNA Blood Purification Kit (Invitrogen, USA). cDNA synthesis was carried out using the PrimeScript II 1st Strand cDNA Synthesis Kit (Takara, Japan). For qPCR, the reaction system was prepared according to the instructions of the TB Green Premix Ex Taq II kit and then the reaction was conducted in the CFX Connect instrument (Bio-Rad, USA). Glyceraldehyde 3-phosphate dehydrogenase (GAPDH) was used for normalization. The primer sequences employed in the qPCR experiment are listed in Table 1.

16S rRNA Analysis

In this study, we used the GenElute Stool DNA Isolation Kit (Sigma-Aldrich) to extract bacterial DNA from human fecal samples. After DNA extraction, we targeted the bacterial 16S rRNA gene V4 variable region and performed PCR amplification using primers 515F-806R with barcode sequences. Subsequently, the PCR products were purified using an AxyPrep DNA Gel Extraction Kit (Corning, USA). Following the purification of the PCR products, we employed the TruSeq DNA PCR-Free kit

(Illumina, USA) to construct MiSeq PE libraries. After library construction, quantification was performed using the Qubit and KAPA Library Quantification Kit (Roche, USA), and high-throughput sequencing was conducted using HiSeq2500 PE 300 (Illumina, USA). First, the raw PE data obtained from the sequencing machine were concatenated and quality controlled to obtain Clean Tags. Subsequently, chimera filtering was performed to obtain Effective Tags that could be used for further analyses. Next, Qiime 2 software (q2cli 2021.2.0; <https://qiime2.org/>) was used to perform operational taxonomic unit (OTU) clustering and species annotation at 0.97 similarity. This process allowed us to align OTU representative sequences with the corresponding microbial database, obtain species classification information for each sample, and annotate them at various taxonomic levels. Based on the clustering results, we conducted α -diversity and β -diversity analyses, and the annotation results provided species composition information at different taxonomic levels.

Metabolomics Analysis

Three times the amount of methanol was supplied to the fecal sample, vortexed, shaken for 5 min, and then centrifuged at 5,000 r/min for 10 min. After that, the supernatant was filtered through a 0.22 μ m filter and analyzed using an Agilent 1290 UHPLC-QTOF-MS system (Agilent, US). For the extraction of rat serum metabolites, the same volume of extraction solution (1:1 methanol: acetonitrile) was used. After ultrasonic treatment for 10 min, the mixture was centrifuged at 12,000 r/min for 15 min and the supernatant was collected for UHPLC-QTOF-MS analysis.

The target compounds were separated by liquid chromatography on a column (2.1 \times 100 mm, 1.7 μ m, Waters ACQUITY UPLC BEH Amide). Phase A consisted of an aqueous solution containing 25 mmol/L ammonium acetate and 25 mmol/L ammonia, whereas Phase B consisted of acetonitrile. Elution conditions were as follows: 0 to 0.5 min, 95% B; 0.5 to 7 min, 95% to 65% B; 7 to 8 min, 65% to 40% B; 8 to 9 min, 40% B; 9 to 9.1 min, 40% to 95% B; 9.1 to 12 min, 95% B. Flow rate of the mobile phase was 0.5 mL/min, and column temperature was maintained at 25°C. Sample tray temperature was set at 4°C, and the injection volume was 2 μ L for both positive and negative ion modes.

We employed a Triple TOF 6600 high-resolution mass spectrometer and acquired data using Information-Dependent Acquisition (IDA) mode. In IDA mode, the data acquisition software (Analyst TF

1.7, AB Sciex) automatically selected ions and collected their corresponding MS/MS data based on the precursor ions detected in the first-level mass spectrometry. For each cycle, 12 of the most intense ions, with intensities greater than 100, were selected for MS/MS scanning. The collision-induced dissociation energy was set at 30 eV, and the cycle time was 0.56 s. The ion source parameters were as follows: GS1, 60 psi; GS2, 60 psi; CUR, 35 psi; TEM, 600°C; DP, 60 V; ISVF, 5000 V (positive ion mode)/-4000 V (negative ion mode). ProteoWizard software was used to convert the raw mass spectrometry data into the mzXML format and then processed using XCMS for retention time correction, peak identification, peak extraction, peak integration, and peak alignment. During the processing, we set the minfrac to 0.5 and cutoff to 0.3. Subsequently, we employed R packages and a secondary mass spectrometry database to identify the peaks of these substances.

Preparation of Fecal Microbiota Suspension

Three HUA-induced ED rats were treated with 37.8 mg/kg of QYHT decoction for 28 days. After gentle abdominal massage to stimulate defecation, the collected feces were weighed and then mixed with approximately five times their weight in physiological saline. The mixture was stirred in a blender, filtered to remove residue, and the resulting suspension was collected. The suspension was transferred to a 10-mL centrifuge tube and centrifuged at 1,200 r/min for 3 min. After removing the supernatant, an equal volume of physiological saline was added to the original suspension, followed by gentle inversion for mixing. This centrifugation and washing process was repeated three times, and the supernatant was discarded, leaving purified fecal microorganisms as a precipitate. To the precipitate, three times its volume of physiological saline was added, and it was gently mixed to obtain the fecal bacterial solution.

Fecal Microbiota Transplantation

Six HUA-induced ED rats were divided into a model group and a fecal transplantation group ($n = 3$ per group). The rats fasted but had access to water after 6:00 p.m. the day before the enema procedure. On the following day, enemas were administered at 8:00 a.m. and 4:00 p.m.. Prior to the enema, gentle massage and stimulation of the rat's abdomen were performed to facilitate expulsion of residual feces. Subsequently, under 2.1% isoflurane, the rats were immobilized in a head-down, tail-up position, and a lubricated enema needle was gently inserted approximately 4 to 5 cm

into the intestinal lumen, followed by slow infusion of the fecal bacterial solution. The enema was retained for 1 min to prevent leakage. After the enema procedure, the rats were released from the fixation and their mental states and activities were observed. If no abnormalities were detected, the rats were returned to their cages and provided with free access to water. After the second enema each day, the rats were allowed free access to food until fasting resumed after 6:00 p.m. on the next day, with water still available. The entire experiment lasted for 5 days, with observations of the rats' activity and blood sample collection on the sixth day.

Non-Targeted Metabolite Detection

LC-MS was used to detect non-targeted metabolites of QYHT decoction in positive and negative ion modes. Metabolites were then identified by comparing the spectral information with the database. Mix the sample, take 100 μ L into a 1.5EP tube, add three times methanol (CNW, Shanghai, China), and vortex for 60 seconds. After ultrasonic treatment for 10 min, the mixture was centrifuged at 17,000g at 20°C for 15 min. Take 100 μ L of the supernatant into the injection bottle and detect it on the machine. The mobile phase column temperature was 40°C and the sample loading volume was 5 μ L.

Statistical Analysis

Statistical analysis and graphing of the data were performed using GraphPad Prism 9.0 software. Student's *t*-test was used for comparisons between two groups, and one-way analysis of variance (ANOVA) was used for comparisons among multiple groups. All data are presented as mean \pm standard deviation (*SD*). A *p*-value of less than .05 was considered statistically significant.

Results

Therapeutic Effect of QYHT Decoction on Patients With HUA-Induced ED

The results of routine blood tests indicated that QYHT reversed the levels of WBC, Hb, HCT, MCH, RBC, MCHC, MPV, PCT, PDW, and PLT in HUA-induced ED patients (shown in Figure 1A). Renal function tests showed that QYHT reduced the levels of γ -GGT, CHOL, CHE, BUN, and BUA in patients with HUA-induced ED (shown in Figure 1B). ELISA results demonstrated that HUA-induced ED patients exhibited enhanced inflammatory and oxidative stress

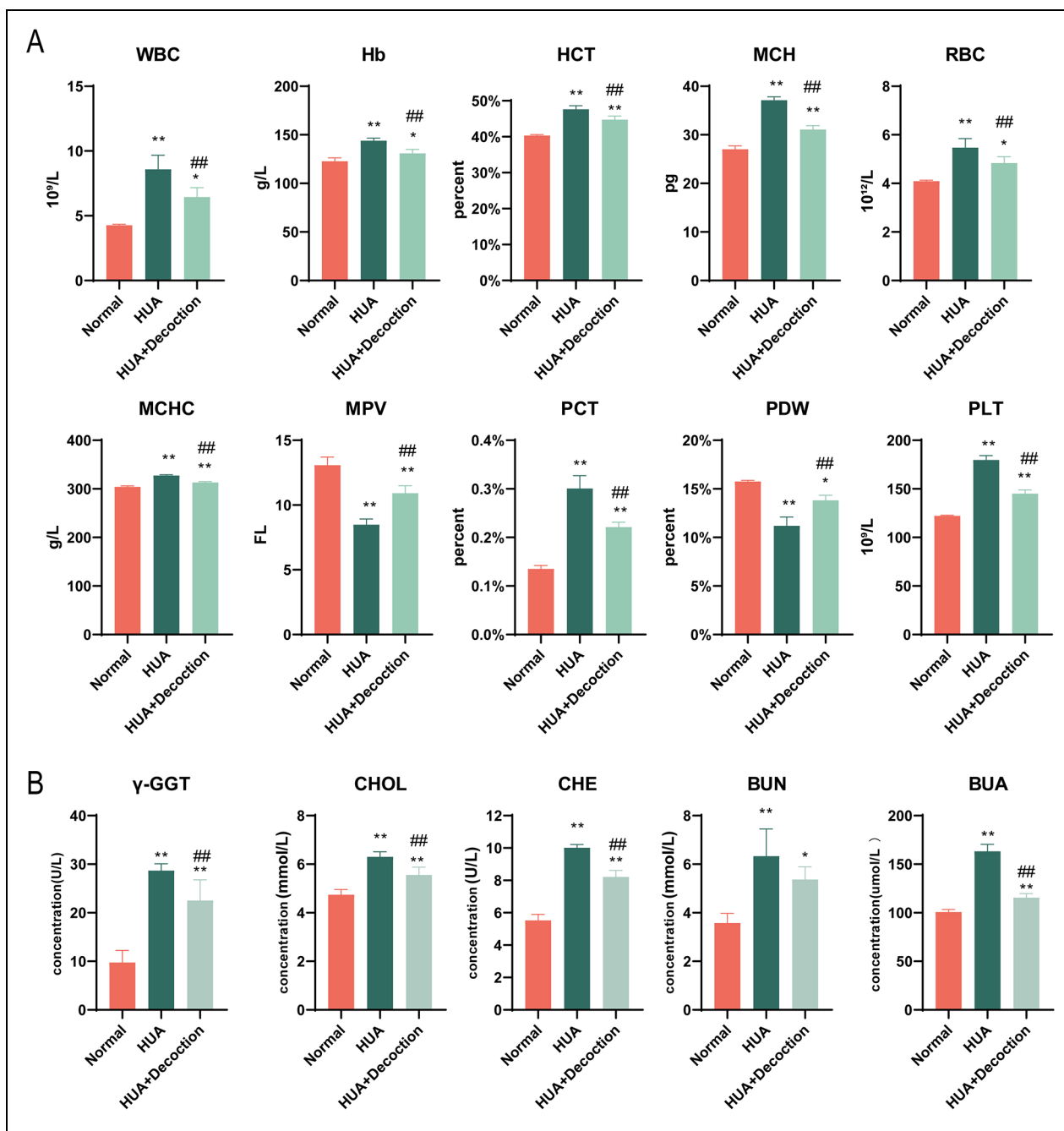


Figure 1. Therapeutic Effects of QYHT on HUA-Induced ED Patients Were Evaluated in This Study

Note. (A) Blood routine examination results. (B) Evaluation of blood biochemical parameters. The values represent the means \pm SDs. One-way analysis of variance (ANOVA) was used for comparisons among multiple groups. As compared to Normal group, ** $p < .01$; as compared to HUA group, ## $p < .01$.

responses, characterized by significant reductions in T and NO levels and significant increases in TNF- α , MDA, CRP, E2, and ET-1 levels, while QYHT decoction reversed these indicators (shown in Figure 2A). To determine the activation of NLRP3 inflammasomes, qPCR was used to test the whole blood of

subjects. The results showed that NLRP3 inflammasomes and their components, ASC and caspase-1, were highly expressed in the blood of patients with HUA ED, and QYHT decoction reduced their expression (shown in Figure 2B). These findings suggest that the QYHT decoction improves liver and kidney

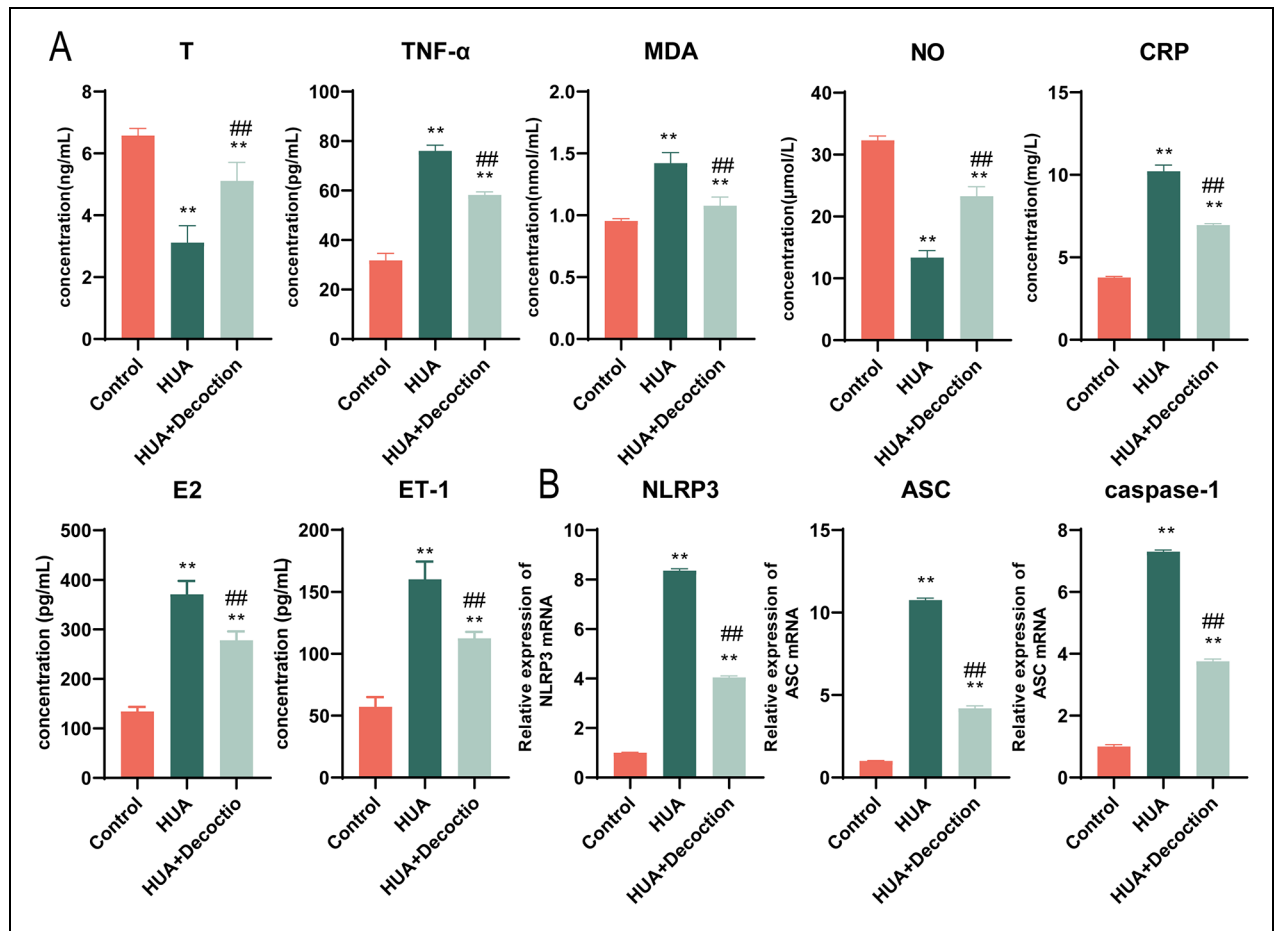


Figure 2. Impacts of QYHT Decoction on Oxidative Stress and Inflammatory Response in HUA-Induced ED Patients

Note. (A) Measurement of T, TNF- α , MDA, NO, CRP, E2, and ET-1 levels in the serum was conducted through ELISA; (B) Assessment of changes in NLRP3, ASC, and caspase-1 levels in whole blood was performed by using qPCR. The values represent the means \pm SDs. One-way ANOVA was used for comparisons among multiple groups. Statistical analysis revealed ** $p < .01$ as compared to normal group, and ## $p < .01$ as compared to HUA group.

function, reduces inflammatory and oxidative stress responses, lowers blood uric acid levels, and promotes erectile function. In addition, HUA-induced ED is associated with NLRP3-mediated inflammatory responses activated by uric acid salt crystals in the blood.

Distribution of Gut Microbiota in HUA-Induced Patients With ED

A dilution curve was used to verify whether the sequencing data was sufficient to reflect species diversity in the samples. As the sequencing volume increased, the dilution curve flattened. The number of microbial species in each group of samples did not significantly increase with the increase in sequencing quantity, indicating that sequencing adequately covered a substantial portion of the

microorganisms in the samples (shown in Figure 3A), making it suitable for data analysis. Results of alpha diversity analysis showed no significant differences in the ACE index, chaol index, and Simpson index among the three groups. However, the Shannon index in the HUA+decoction group was significantly higher than that in the HUA group (shown in Figure 3B), suggesting that the QYHT decoction increases the diversity of the gut microbiota in patients with HUA. Based on PCoA analysis, samples from each group were completely separated, and samples from the same group clustered together, indicating that the microbial composition between samples in each group was similar (shown in Figure 3C). PC1 and PC2 of the PCoA explain 14.16% and 11.77% of the total variance, respectively. Samples from the HUA+decoction and HUA groups were largely

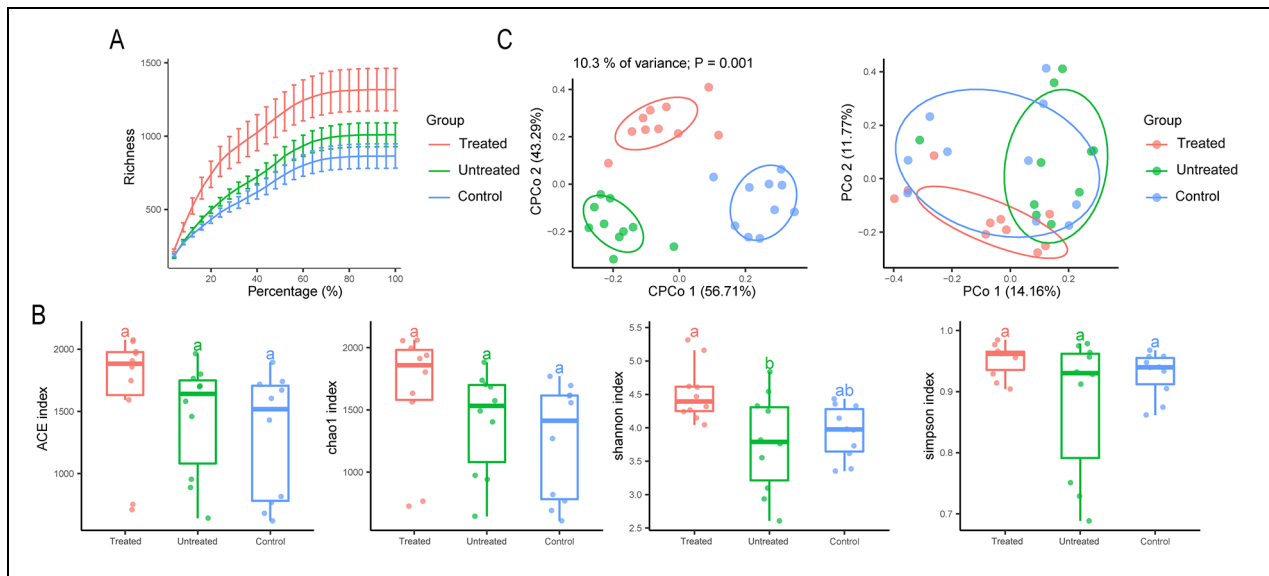


Figure 3. Impacts of QYHT on Gut Microbiota Diversity in HUA-Induced ED Patients

Note. (A) Dilution curve; (B) Box plot of alpha diversity; and (C) Beta diversity analysis. FY: QYHT + HUA group. WFY: HUA group. The letters "a/b" in B denote the letter marking method for significant differences. Same letters indicate no significant differences between the groups, while different letters indicate significant differences. One-way ANOVA was used for comparisons among multiple groups.

separated, indicating that the composition of the gut microbiota in HUA patients changed after the QYHT decoction treatment (shown in Figure 3C).

In the analysis of fecal samples from the Control, HUA with comorbid ED, and HUA + decoction groups, we identified 137, 126, and 131 OTUs, respectively (shown in Figure 4A). At the phylum level, the predominant bacterial groups were Firmicutes, Bacteroidetes, Proteobacteria, Actinobacteria, Verrucomicrobia, Acidobacteria, and Gemmatimonadetes. In contrast to the control group, the HUA group showed a decrease in Actinobacteria abundance, but an increase in Verrucomicrobia (shown in Figure 4B). In contrast, the HUA + decoction group exhibited a higher abundance of Firmicutes, Bacteroidetes, and Acidobacteria than the HUA group, whereas Proteobacteria abundance was reduced. At the class level, the main bacterial groups identified were Clostridia, Bacteroidia, Gammaproteobacteria, Bacilli, Actinobacteria, Verrucomicrobiae, and Erysipelotrichia. The abundance of Clostridia, Bacteroidia, and Erysipelotrichia was higher in the HUA group, whereas Gammaproteobacteria abundance was lower. At the order level, the HUA group showed an increased abundance of Pseudomonadales and Verrucomicrobiales than the Control and HUA + QYHT groups, while the HUA + decoction group exhibited a higher abundance of Clostridiales and Bacteroidales compared to the

HUA group, with a decrease in Enterobacteriales. At the family level, the bacterial families detected included Lachnospiraceae, Bacteroidaceae, Ruminococcaceae, Prevotellaceae, Enterobacteriaceae, Pseudomonadaceae, and Peptostreptococcaceae. Although these three groups shared similar microbial compositions, the HUA + decoction group showed a higher abundance of Lachnospiraceae, Bacteroidaceae, Ruminococcaceae, Prevotellaceae, and Peptostreptococcaceae than the HUA group, while Enterobacteriaceae and Pseudomonadaceae were less abundant. At the genus level, Bacteroides, Prevotella_9, Faecalibacterium, Pseudomonas, Blautia, Escherichia-Shigella, and Lachnospiraceae were detected. The HUA + decoction group showed a lower abundance of Bacteroides, Prevotella_9, Faecalibacterium, and Blautia than the HUA group, while Pseudomonas, Escherichia-Shigella, and Lachnospiraceae also exhibited decreased abundance.

Through LDA and LefSe analyses, we identified significant differences in microbial species among the various groups. Significantly different species in the control group included Enterobacteriaceae, Enterobacteriales, Actinobacteria, Bifidobacterium, Bifidobacteriaceae, Bifidobacteriales, Actinobacteria, and Catenibacterium. Significantly different species in the HUA group were Proteobacteria, Gammaproteobacteria, Akkermansia, Verrucomicrobia, Verrucomicrobiae, Verrucomicrobiales, Verrucomicrobiaceae,

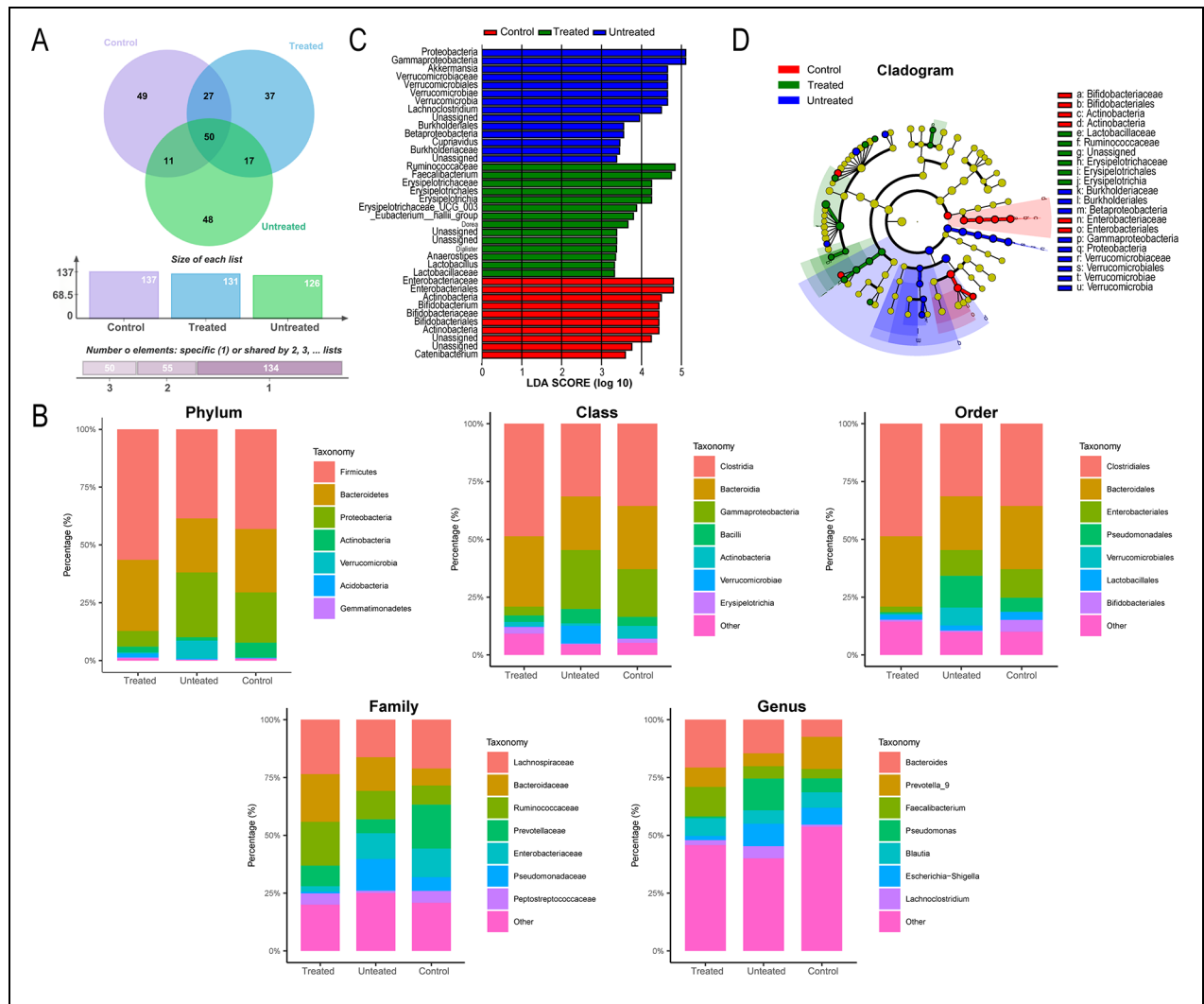


Figure 4. Impacts of QYHT Decoction on the Gut Microbiota Composition of HUA-Induced ED Patients Was Investigated
 Note. (A) OTU clustering analysis; (B) Gut microbiota composition analysis at various taxonomic levels; and (C and D) LefSe analysis.

Burkholderiaceae, Cupriavidus, Betaproteobacteria, Burkholderiales, and Lachnospirillum. In the HUA + decoction group, the significantly different species were Lactobacillaceae, Lactobacillus, Anaerostipes, Dialister, Dorea, Eubacterium_hallii_group, Erysipelotrichaceae_UCG_003, Erysipelotrichia, Erysipelotrichales, Erysipelotrichaceae, Faecalibacterium, and Ruminococcaceae (shown in Figure 4C and D).

Through *Phylogenetic Investigation of Communities by Reconstruction of Unobserved States* (PICRUST) functional prediction analysis, significant differences in Kyoto Encyclopedia of Genes and Genomes (KEGG) metabolic pathways were observed between the different groups. The differentially abundant microbial pathways between the

control group and HUA + decoction group were mainly related to lipid ($p = .000878$), carbohydrate ($p = .012$), and amino acid metabolism ($p = .034$) (shown in Figure 5A). In contrast, the main differential microbial pathways between the Control and HUA groups were associated with the following protein families: metabolism ($p = .019$) and nucleotide metabolism ($p = .036$) (shown in Figure 5B). Finally, the differential microbial pathways between the HUA + decoction and HUA groups primarily involved energy metabolism ($p = .01$), protein families: metabolism ($p = .011$), protein families: genetic information processing ($p = .012$), and protein families: signaling and cellular processes ($p = .025$) (shown in Figure 5C).

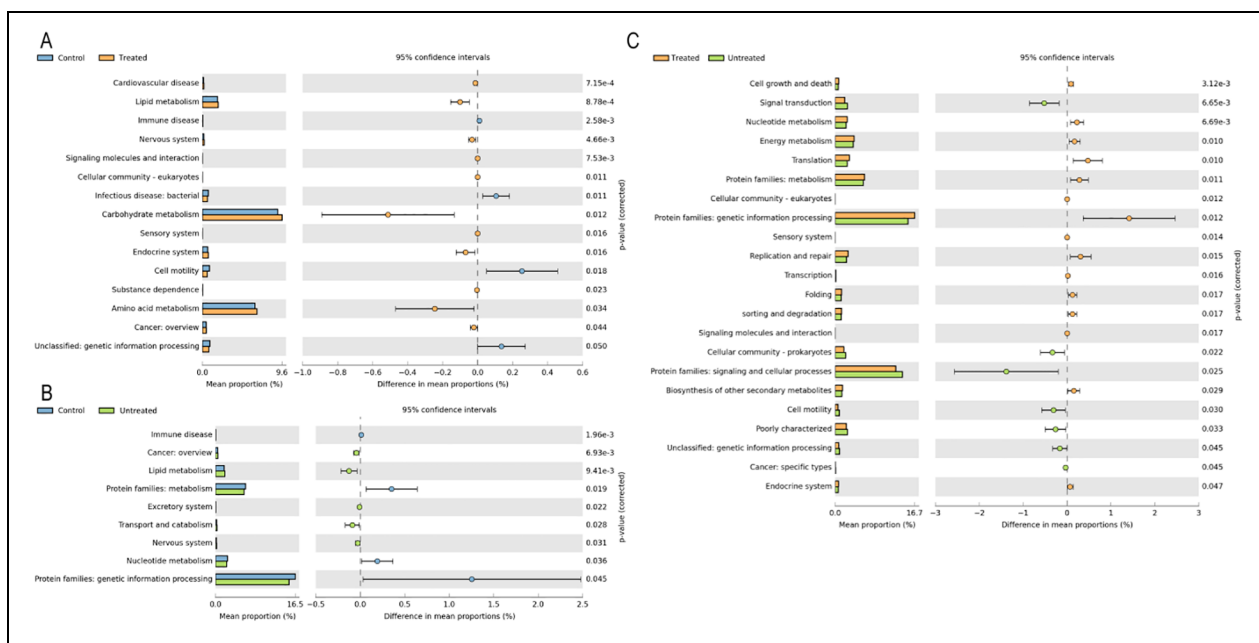


Figure 5. Impacts of QYHT on KEGG Metabolic Pathways of the Gut Microbiota in HUA-Induced Patients With ED Was Studied Note. Comparisons A, B, and C represent the contrasts between Control and HUA+decoction, Control and HUA, and HUA and HUA+decoction groups, respectively.

Analysis Onto the Fecal Metabolites in HUA-Induced ED Patients

PCA results displayed the sample distribution between the untreated and treated groups. The principal component differences between the Ex and HE group samples were not significant (shown in Figure 6A). Next, partial least squares discrimination analysis (PLS-DA) was employed to evaluate the accuracy of model construction. Based on 200 permutations and modeling, the regression line values (R^2) for all groups were found to be greater than the Q^2 values. Moreover, the Q^2 regression line intersected the Y-axis at a value less than 0, indicating that the model did not overfit and was an effective predictive model with good stability and prediction capability (shown in Figure 6B). Differential analysis of the detected metabolites was conducted using the criteria of variable importance in the projection (VIP) >1.0 , fold change (FC) >1.2 , FC <0.833 , and p -value $<.05$. This screening yielded 23 upregulated and 75 downregulated metabolites (shown in Figure 6C). Hierarchical cluster analysis was performed on the differentially expressed metabolites from both groups, revealing differences in the metabolic expression patterns between the groups and within each group (shown in Figure 6D). In addition, a comparative display of the top 20 upregulated and downregulated metabolites based on \log_2 FC ratios

provided a more intuitive understanding of metabolites with significant differences (shown in Figure 6E). Further KEGG analysis revealed that these differentially expressed metabolites were involved in signaling pathways such as protein digestion and absorption, lysine degradation, and beta-alanine metabolism (shown in Figure 6F).

Impacts of QYHT Decoction on HUA-Induced ED Rats

After the 57th day of modeling, blood samples were collected from the rats to examine the levels of UA, BUN, and Cr to verify the successful establishment of the rat HUA model. Our results revealed significantly elevated levels of UA, BUN, and Cr in the model group compared with those in the control group, indicating the successful establishment of the HUA model (shown in Figure 7A). QYHT led to a marked dose-dependent reduction in NLRP3, ASC, and caspase-1 levels in rats (shown in Figure 7B). In addition, following a 28-day treatment with QYHT, the levels of T and NO significantly increased in HUA-induced ED rats, whereas the levels of CRP, MDA, TNF- α , E2, and ET-1 significantly decreased (shown in Figure 7C). These findings suggest that QYHT ameliorates HUA-induced ED symptoms by reducing the inflammatory and oxidative stress responses.

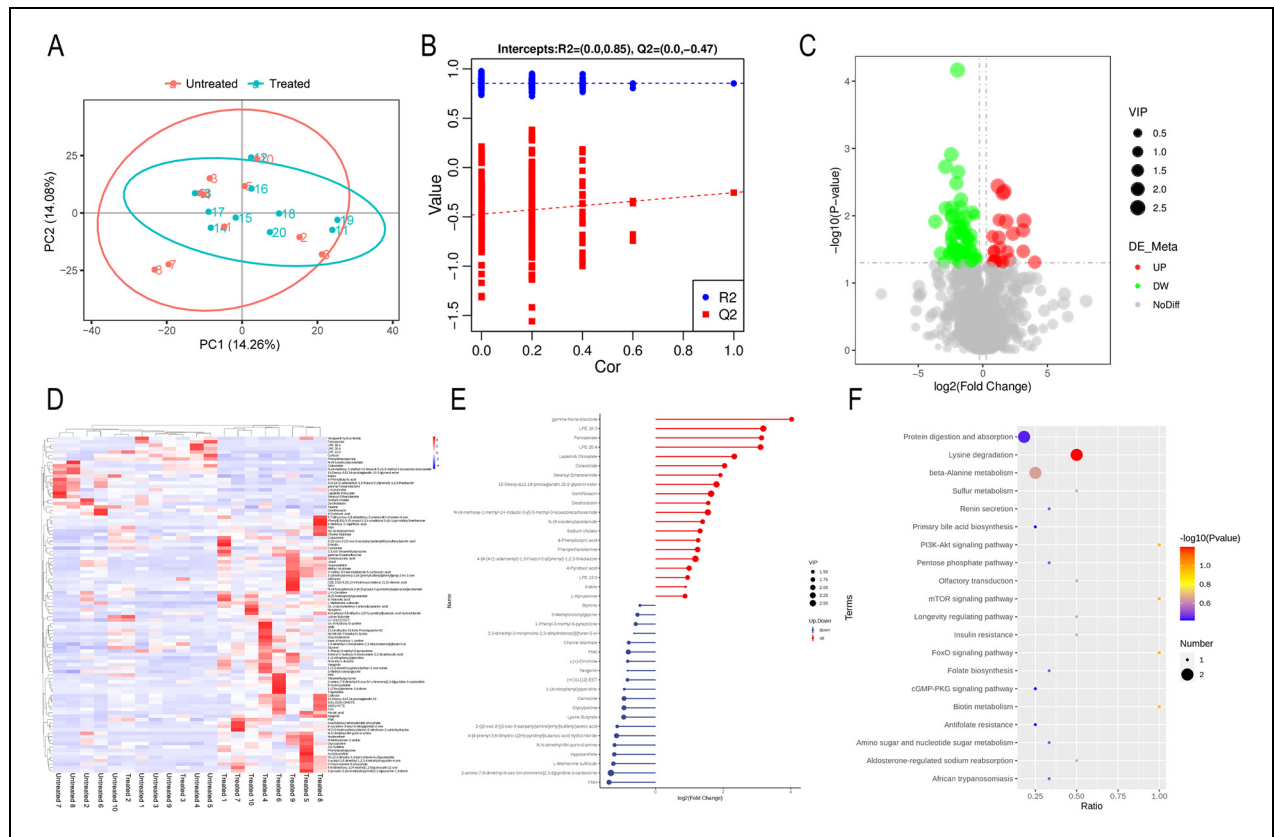


Figure 6. Impacts of QYHT Decoction on Fecal Metabolites of HUA-Induced ED Patients

Note. (A) PCA results; (B) PLS-DA validation results; (C) volcano plot of differential metabolites; (D) Heatmap of differential metabolites clustering; (E) bar graph illustrating the top 20 upregulated and downregulated differential metabolites; and (F) KEGG enrichment results of differential metabolites.

Impacts of QYHT Decoction on the Serum Metabolites of HUA-Induced ED Rats

During the comparative study, we also conducted a metabolomic analysis of serum from the QYHT and model groups. Our results showed that the sample distribution in the QYHT group was similar, indicating similarities in the types and levels of metabolites within the group (shown in Figure 8A). Furthermore, through OPLS-DA analysis, we observed a significant separation between the two groups along the t[1]P coordinate, suggesting distinct principal components between the groups (shown in Figure 8B). Among these two groups, 55 differentially expressed metabolites were identified, with nine upregulated and 46 downregulated metabolites (shown in Figure 8C). By matching with the secondary mass spectrometry database, we successfully identified seven metabolites, namely 1-Methylnicotinamide, 3-Hydroxyanthranilic acid, Phenacetine, Ser-Gly, 3-(3-Indolyl)-2-oxopropionic acid, Glu-Pro, and Honokiol (shown in

Figure 8D). In the QYHT group, Phe and Ser-Gly were upregulated, while 1-Methylnicotinamide, 3-Hydroxyanthranilic acid, 3-(3-Indolyl)-2-oxopropionic acid, Glu-Pro, and Honokiol were downregulated (shown in Figure 8E). Further KEGG annotation results indicated that these seven differentially expressed metabolites were associated with the nicotinate and nicotinamide metabolism and tryptophan metabolism pathways (shown in Figure 8F).

Impacts of Fecal Microbiota Transplantation on HUA-Induced ED Rats

After treatment with fecal microbiota transplantation (FMT), the T content in HUA-induced ED rats significantly increased, while the levels of CRP, MDA, NO, TNF- α , E2 and ET-1 decreased (shown in Figure 9A). Furthermore, FMT inhibited NLRP3 activation, leading to a significant reduction in the mRNA expression levels of NLRP3, ASC, and caspase-1 (shown in Figure 9B).

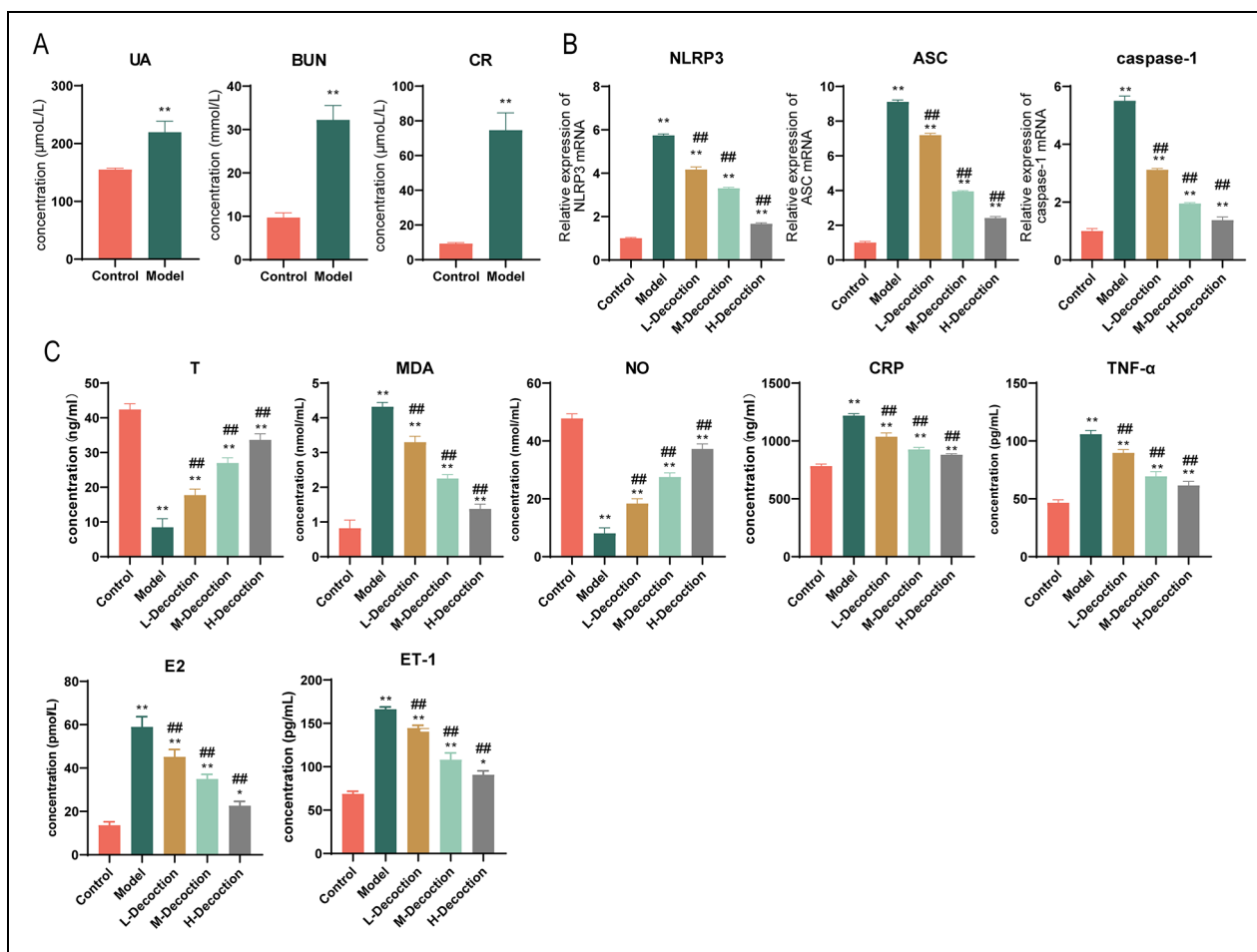


Figure 7. Impacts of QYHT Decoction on Oxidative Stress Response and Inflammatory Reaction in HUA-Induced ED Rats
 Note. (A) Verification of the HUA rat model by assessing the levels of UA, BUN, and CR; (B) qPCR analysis onto the changes in NLRP3, ASC, and caspase-1 in the serum of HUA-induced ED rats; (C) ELISA assessment of T, TNF-α, MDA, NO, CRP, E2, and ET-1 levels in the serum of HUA-induced ED rats. The values represent the means \pm SDs. One-way ANOVA was used for comparisons among multiple groups. Statistical comparisons: ** $p < .01$ versus Control group; ## $p < .01$ versus Model group.

The Molecular Docking Analysis Combined With Network Pharmacology

We performed an intersection analysis between individual components and disease targets from the Genecards database, encompassing a total of 444 disease targets; the drug component targets amounted to 625. Following the integration of the compounds and disease targets, we identified 95 common gene targets (shown in Figure 10A). Visualizing these intersecting genes and active molecules in a network graph revealed a correlation between 42 drug component targets and these intersecting genes (shown in Figure 10B). Subsequently, we constructed a Protein-Protein Interaction (PPI) network to analyze potential protein interactions. Genes such as AKT1, TNF, TP53, and JAK2 occupied central positions in this network, having the most connections, thereby serving

as candidate genes or signaling pathways for further research (shown in Figure 10C). To elucidate the functionality of the primary component targets and the role of potential targets in signaling pathways, we conducted gene ontology (GO) analysis (shown in Figure 10D) and ranked the top 30 pathways through KEGG analysis (shown in Figure 10E) for the 95 targets. The visualization of the enrichment analysis results indicated 3,968 biological processes (BP), 265 cellular components (CCs), and 432 molecular functions (MFs). Among the top 10 enrichments, BPs were mainly involved in response to xenobiotic stimulus, response to oxygen levels, and positive regulation of kinase activity. CCs were primarily associated with membrane rafts, membrane microdomains, and vesicle lumen, whereas MFs mainly participated in nuclear receptor activity, ligand-activated transcription factor activity, and

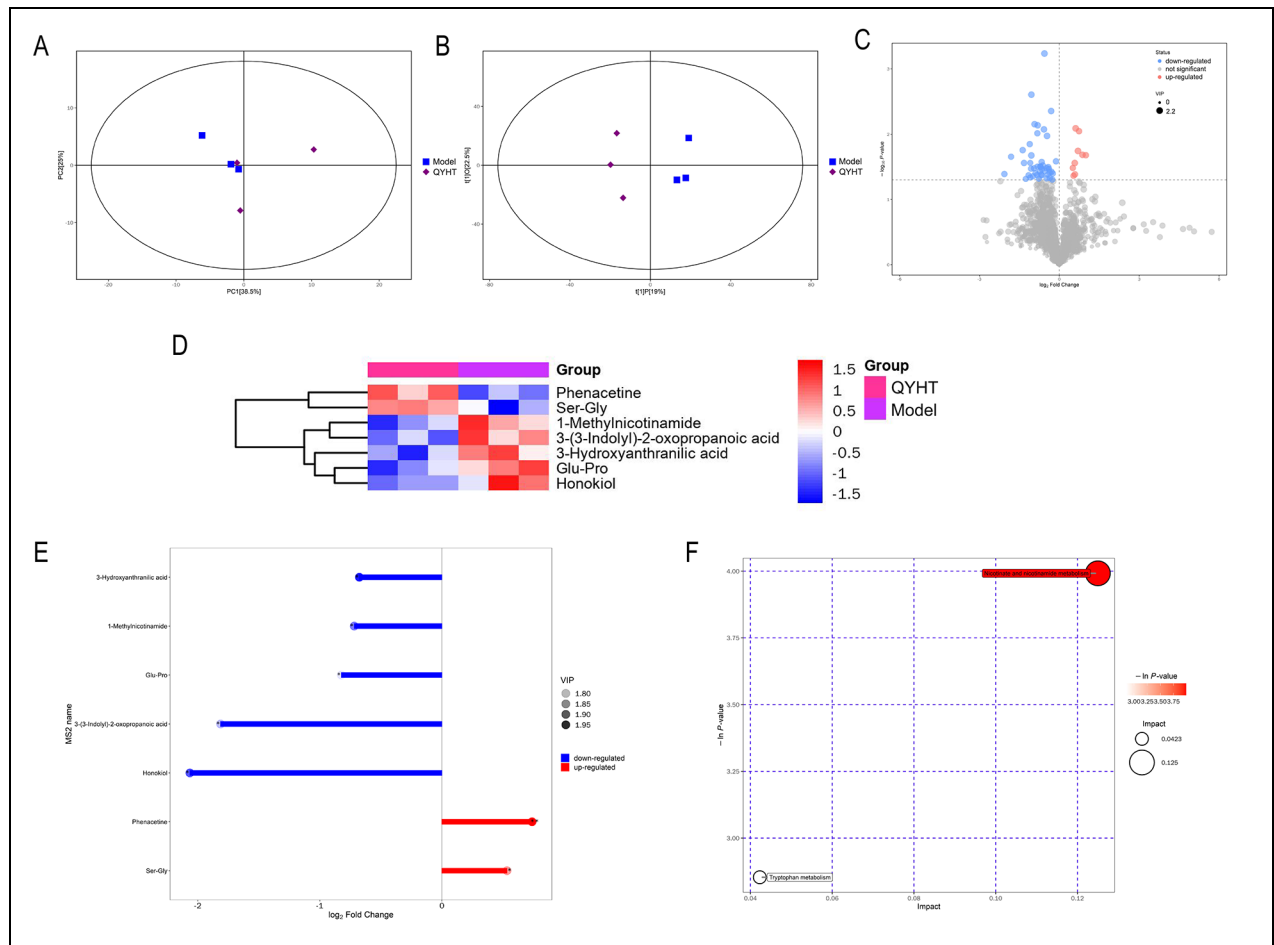


Figure 8. Impacts of QYHT Decoction on the Serum Metabolites of HUA-Induced ED Rats

Note. (A) PCA results; (B) OPLS-DA results; (C) volcano plot of differentially expressed metabolites; (D) hierarchical clustering heatmap of differentially expressed metabolites; (E) metabolic pathway enrichment analysis of differentially expressed metabolites; and (F) bar plot depicting the fold changes of differentially expressed metabolites.

protein serine/threonine/tyrosine kinase activity. Notable pathways in the KEGG enrichment included diabetic cardiomyopathy, the PI3K-Akt signaling pathway, and AGE-RAGE signaling pathway in diabetic complications. Research shows that JAK2 deficiency can improve ED in diabetic mice (Li et al., 2021) and alleviate HUA (Zhang et al., 2023). In addition, there have been many reports showing that the JAK2/STAT3 pathway is closely linked to the activation of the NLRP3 inflammasome (Cao et al., 2020; Xiao et al., 2022). By combining the results of network pharmacology research with those of previous studies, JAK2 drew our attention. Consequently, we employed molecular docking to validate the accuracy and reliability of the interactions between JAK2 and its key components. These results indicated binding interactions between JAK2 and mandenol from Coix seed and linoleyl acetate from Epimedium, with binding energies of -5.7

kcal/mol and -5.5 kcal/mol, respectively (shown in Figure 10F).

Partial Mass Spectrum Information of QYHT Decoction

In order to identify the component types of QYHT decoction, we used LC-MS in positive and negative ion modes to detect non-targeted metabolites of QYHT and compared the spectral information with the database for metabolite identification. Partial mass spectrum information of QYHT decoction was listed in Supplementary Table 1. The total ion current of the sample TIC is shown in Figure 11.

Discussion

Penile erection is controlled by neurovascular regulation and closely associated with the NO/cGMP

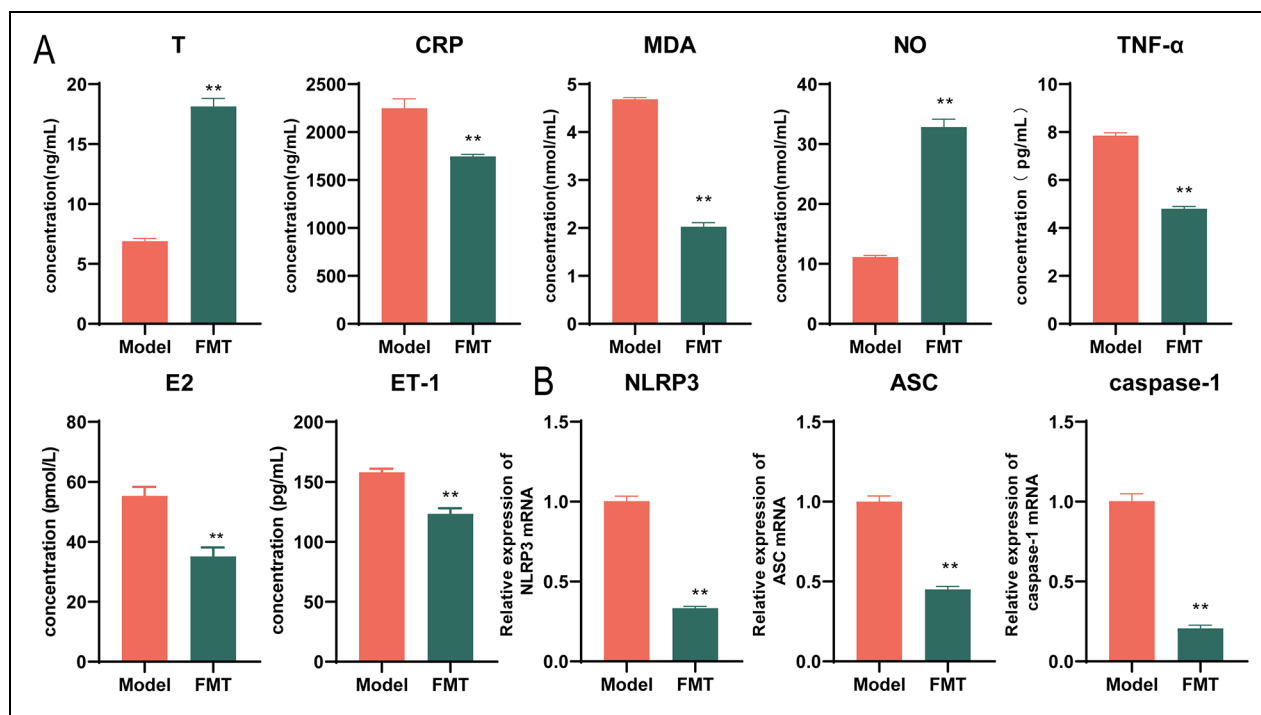


Figure 9. Impact of FMT on Oxidative Stress and Inflammatory Responses in HUA-Induced ED Rats

Note. (A) ELISA measurement of serum levels of T, TNF- α , MDA (malondialdehyde), NO (nitric oxide), CRP (C-reactive protein), and E2 (estradiol) and ET-1 (endothelin-1); (B) qPCR analysis of changes in NLRP3, ASC, and caspase-1 expression in whole blood. The values represent the means \pm SDs. Student's *t*-test was used for comparisons between two groups. ***p* < .01 indicates the statistical significance compared to model group.

pathway. Upon sexual stimulation, non-cholinergic and non-adrenergic nerve terminals release neurotransmitters, activating neuronal nitric oxide synthase (nNOS) in nerves and endothelial nitric oxide synthase (eNOS) on the endothelial cells of the corpus cavernosum, leading to the production of nitric oxide (NO). This process is mediated through the NO/cGMP signaling pathway, causing relaxation of the penile smooth muscles, vasodilation, and engorgement of blood, thereby facilitating and maintaining penile erection. Vascular endothelial cells are able to secrete NO, ET, and angiotensin to collectively regulate vascular and corpus cavernosum smooth muscle relaxation and contraction. However, excessive levels of uric acid directly inhibit the synthesis of eNOS, leading to reduced NO release, which is also the reason for the more severe vascular endothelial and smooth muscle damage in patients with ED compared with those without ED (Kato et al., 2005). The severity of endothelial dysfunction in patients with HUA is positively correlated with serum uric acid levels (Yavuzgil et al., 2005). In addition, previous literature reported that the expression of E2 and T is closely related to sexual function. When the E2/T ratio increases, the erectile function of the penis decreases, that is, it is negatively correlated (Pan et al., 2020).

Under normal circumstances, uric acid exists in a soluble form as urate salts, and its synthesis and excretion maintain a dynamic balance. In addition, uric acid serves as an antioxidant and anti-inflammatory agent, protecting vascular endothelial cells from oxidative stress and inflammation. However, excessive intake of purines, metabolic disorders, or enzyme abnormalities can lead to elevated serum uric acid levels. When uric acid levels exceed 408 $\mu\text{mol/L}$, urate crystals form and activate NLRP3 inflammasome (Correa-Costa et al., 2011; Jin et al., 2012). The NLRP3-mediated inflammatory response is a significant factor in endothelial dysfunction caused by high uric acid levels (Hou et al., 2022; Xing et al., 2019). Under normal physiological conditions, pro-caspase-1 remains in an inactive state. Upon activation of the NLRP3 inflammasome, pro-caspase-1 is processed and activated into active caspase-1, which then cleaves the precursor of IL-1 β and IL-18, resulting in the generation and release of IL-1 β and IL-18. This triggers the recruitment of inflammatory factors, leading to inflammation infiltration (Ising et al., 2019; Latz et al., 2013). Knocking out NLRP3 inflammasome or inhibiting NLRP3 with drugs significantly reduces the release of pro-inflammatory cytokines TNF- α and IL-1 β , thereby alleviating endothelial damage and vascular dysfunction (Lv et al., 2023; Mulay et al., 2013).

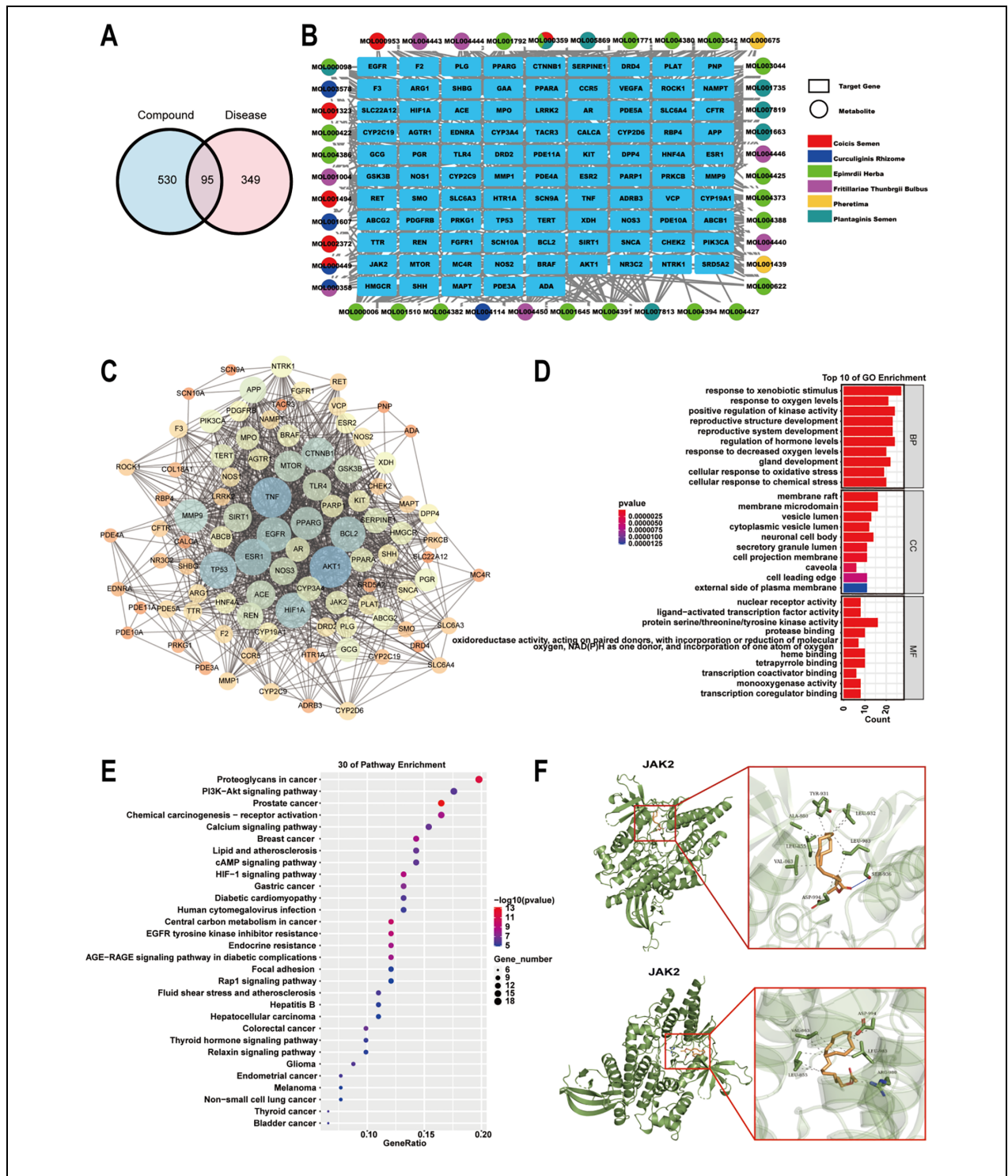


Figure 10. Network Pharmacology Analysis and Molecular Docking Onto the Relevance Amid QYHT Decoction and HUA-Induced ED

Note. (A) Molecular-disease target intersection gene Venn diagram. (B) Network graph of active ingredient-target gene interactions: 95 targets from 42 major active ingredients within the intersection genes. (C) Protein-protein interaction network analysis. (D) Diagram of intersection gene GO analysis: The left Y-axis represents the GO pathway names, the X-axis represents the GeneRatio values, and each functional category identifies the top 10 enriched pathways. (E) Bubble chart of intersection gene KEGG analysis: Identifying the top 30 enriched pathways. The size of each circle represents the number of genes matched to that pathway, with larger circles indicating more matched genes. The color depth indicates smaller p-values. (F) JAK2 binding with mandenol (above) and JAK2 binding with linoleyl acetate (below).

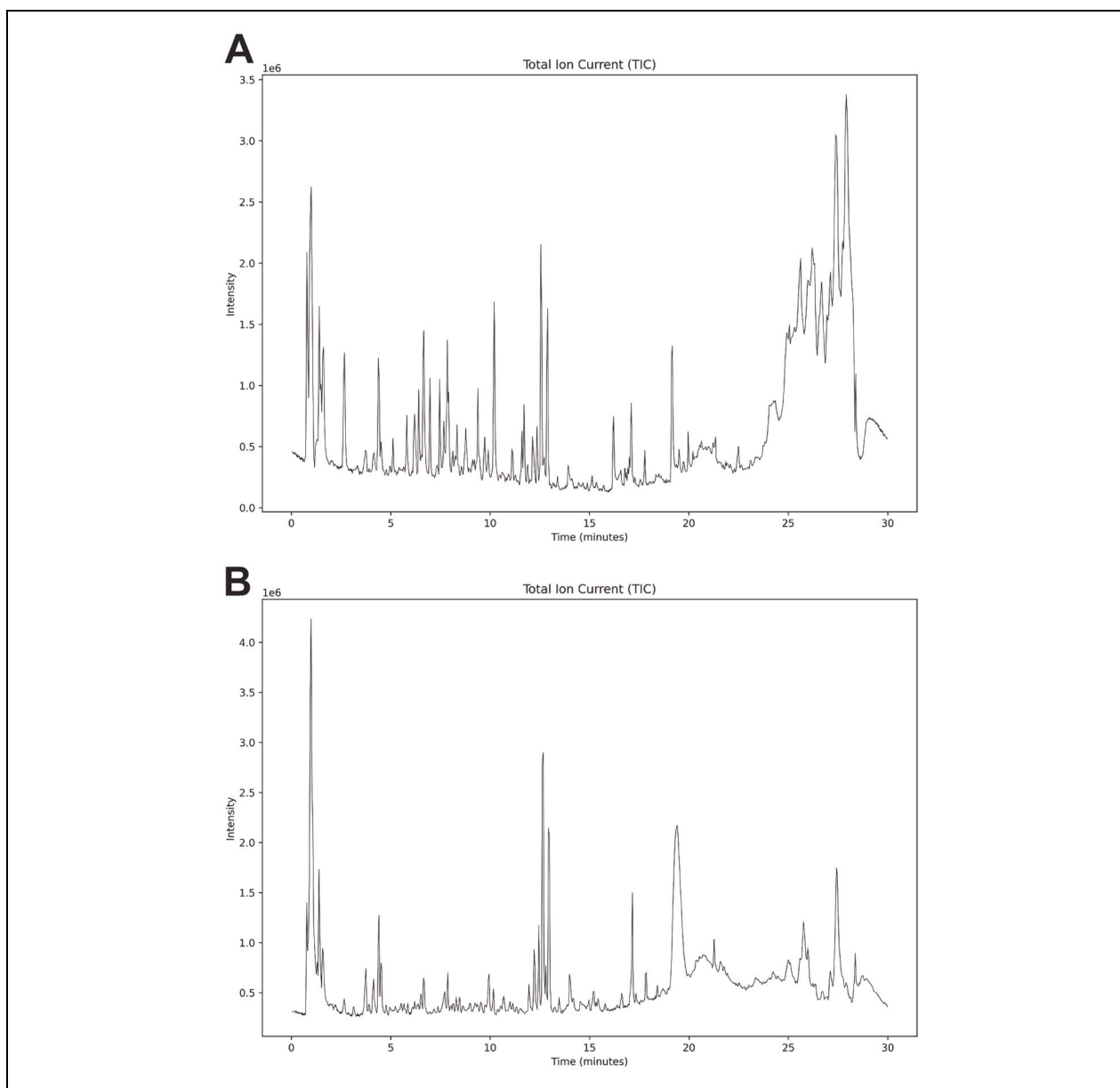


Figure 11. TIC Total Ion Current Diagram of QYHT Decoction

Note. (A) Positive ion mode TIC graph. (B) Negative ion mode TIC chart.

In the treatment of ED, phosphodiesterase type 5 (PDE-5) inhibitors, represented by Sildenafil, remain the first-line therapeutic option, working by increasing NO levels, leading to smooth muscle relaxation and improvement in erectile function (Roumeguère et al., 2003). However, for certain patients, especially the elderly, the efficacy of Sildenafil is often limited. Elderly patients typically exhibited a decline in physiological function with multiple comorbidities, which reduced their ability to metabolize medications, increasing the risk of adverse drug reactions.

Dopamine receptor agonists also promote erectile response by stimulating the central nervous system, but their therapeutic effect is relatively mild (Kolasa et al., 2006). Traditional Chinese medicine has shown potential therapeutic value in the prevention and treatment of ED, and its efficacy for ED treatment has also been recognized by several studies (Feng et al., 2022; Seo et al., 2015; Wu et al., 2023). In addition, our previous study has found that QYHT can improve penile hemodynamics and endothelial function in patients with HUA, thereby restoring erectile function (Ge

et al., 2018; Ge & Guo, 2020). In rat model, it was found that QYHT might improve erectile function by inhibiting the inflammatory response mediated by the NLRP3 inflammasome, thereby alleviating vascular endothelial damage. In this study, we sought to explore the underlying mechanisms of QYHT decoction in the treatment of HUA-induced ED.

We found that QYHT decoction effectively increased T levels in patients or rats with HUA-induced ED, while reducing the levels of NLRP3, ASC, caspase-1, TNF- α , MDA, NO, CRP, E2, and ET-1. Further analysis revealed that QYHT decoction altered the gut microbiota distribution in HUA patients, leading to an increase in the abundance of Firmicutes, Bacteroidetes, and Acidobacteria, and a decrease in Proteobacteria. Activation of NLRP3 inflammasome was closely associated with intestinal barrier integrity, microbial composition, and gut metabolites. On one hand, the NLRP3 inflammasome had a regulatory effect on gut microbiota. Studies, such as by Elinav et al., found that NLRP3 $^{-/-}$ mice exhibited an abnormal gut microbial community with increased Prevotellaceae and decreased Lactobacillaceae (Chen et al., 2016). NLRP3 $^{-/-}$ mice were more susceptible to colitis, mainly due to reduced expression of anti-inflammatory cytokines IL-10 and transforming growth factor β 1 induced by IL-1 β (L. Liu et al., 2020). Macrophages isolated from the peritoneal cavity of NLRP3 $^{-/-}$ mice showed no response to bacterial cell wall dipeptides, and neutrophils displayed significantly decreased chemotactic activity and enhanced spontaneous cell apoptosis. Moreover, NLRP3 $^{-/-}$ mice exhibited reduced expression of colonic β -defensin and antimicrobial secretions, while the abundance of Enterobacteriaceae and segmented filamentous bacteria increased (L. Liu et al., 2020). On the other hand, the gut microbiota could also activate the NLRP3 inflammasome. For example, pathobiont *Proteus mirabilis* of the Enterobacteriaceae family induced IL-1 β release through NLRP3 inflammasome, aggravating intestinal damage (Xu et al., 2022). However, *Lactobacillus rhamnosus* GR-1 could reduce the expression of NLRP3 inflammasome and caspase-1 induced by *Escherichia coli*, improve cell morphology and ultrastructure, and reduce inflammation caused by *E. coli* (Huang et al., 2018). Furthermore, *Bifidobacterium longum*, *Bacteroides fragilis*, and adherent-invasive *E. coli* were also confirmed to activate the NLRP3 inflammasome, exacerbating intestinal inflammation (Chen et al., 2016; De la Fuente et al., 2014).

In addition, we found that alterations in gut microbiota abundance have an impact on the metabolism

and degradation of lysine, beta-alanine, and tryptophan. During the inflammatory process, amino acids play a role in the growth, proliferation, and functional regulation of immune cells. Certain amino acids are believed to possess anti-inflammatory properties, regulating the activity of white blood cells, reducing inflammatory responses, and promoting wound healing and tissue repair. Research indicated that specific inhibitors of lysine acetyltransferase can block the activation of NLRP3 inflammasome (L. Liu et al., 2020). Beta-alanine exhibited a positive correlation with the expression of iNOS, IL-1 β , and IL-6 (Xu et al., 2022). Disruptions in tryptophan metabolism are also associated with the activation of the NLRP3 inflammasome and inflammatory responses, as metabolites of tryptophan could promote NLRP3 oligomerization in an ATP-independent manner, thus exerting therapeutic effects against NLRP3-mediated diseases (Huang et al., 2018). These findings suggested that lysine, beta-alanine, and tryptophan may directly or indirectly influence the activation of the NLRP3 inflammasome.

In summary, our findings demonstrate that QYHT decoction can alleviate symptoms of ED induced by HUA in both patients and rats by regulating the abundance of gut microbiota, influencing amino acid metabolism, and thereby modulating the formation of NLRP3 inflammasomes and the release of inflammatory mediators. However, there are still several limitations that should be acknowledged. Although our study has identified the key role of NLRP3 in QYHT treatment of ED induced by HUA, it was limited to preliminary detections, lacking further validation through animal and cellular experiments. Therefore, in our future research, a HUA-induced ED model can be established and treated with QYHT decoction, in combination with NLRP3 knockout or overexpression models, to evaluate whether the activation of NLRP3 is closely related to ED, and explore how QYHT regulates intestinal flora to inhibit the activation of NLRP3.

Conclusion

In conclusion, this study has found that QYHT decoction effectively inhibits the activation of NLRP3 inflammasome and improves penile erectile function by regulating gut microbiota distribution and amino acid metabolism. In addition, it successfully reduces oxidative stress and inflammatory response levels. This decoction offers a novel therapeutic approach for treating ED caused by HUA.

Author Contributions

PG: Conceptualization, Writing – original draft; YG: Data curation, Formal analysis; BC: Methodology; HJ: Validation; LC: Visualization; ZC: Software; KT: Writing – review and editing. All authors contributed to the important editorial changes in the manuscript. All authors read and approved the final manuscript.

Declaration of Conflicting Interests

The author(s) declared no potential conflicts of interest with respect to the research, authorship, and/or publication of this article.


Funding

The author(s) disclosed receipt of the following financial support for the research, authorship, and/or publication of this article: This study was supported by the Guizhou Administration of Traditional Chinese Medicine (grant number QZYY-2024-026), and the Science and Technology Foundation of Guizhou Province (grant number ZK [2021] General 507).

Ethics Approval and Consent to Participate

The research protocol was reviewed and approved by the Ethics Committee of the First Affiliated Hospital of Guizhou University of Traditional Chinese Medicine (Approval No. K2021-004). All experiments were performed in accordance with relevant guidelines and regulations such as the Declaration of Helsinki and the parents signed the informed consent form and agreed to be published. Also, all experimental protocols were approved by the Animal Ethics Committee of the First Affiliated Hospital of Guizhou University of Traditional Chinese Medicine. All methods were carried out in accordance with relevant guidelines and regulations. All methods are reported in accordance with ARRIVE guidelines.

ORCID iD

Kaifa Tang  <https://orcid.org/0009-0000-5985-7824>

Data Availability Statement

All data generated or analyzed during this study are included in this published article.

Supplemental Material

Supplemental material for this article is available online.

References

Becker, B. F., Reinholz, N., Leipert, B., Raschke, P., Permannetter, B., & Gerlach, E. (1991). Role of uric acid as an endogenous radical scavenger and antioxidant. *Chest*,

100(Suppl. 3), 176S–181S. https://doi.org/10.1378/chest.100.3_suppl.176S

Calzo, J. P., Austin, S. B., Charlton, B. M., Missmer, S. A., Kathrins, M., Gaskins, A. J., & Rich-Edwards, J. W. (2021). Erectile dysfunction in a sample of sexually active young adult men from a U.S. cohort: Demographic, metabolic, and mental health correlates. *Journal of Urology*, 205(2), 539–544. <https://doi.org/10.1097/JU.0000000000001249>

Cao, F., Tian, X., Li, Z., Lv, Y., Han, J., Zhuang, R., & Zhou, Z. (2020). Suppression of NLRP3 inflammasome by erythropoietin via the EPOR/JAK2/STAT3 pathway contributes to attenuation of acute lung injury in mice. *Frontiers in Pharmacology*, 11, Article 306. <https://doi.org/10.3389/fphar.2020.00306>

Chen, K., Shanmugam, N. K., Pazos, M. A., Hurley, B. P., & Cherayil, B. J. (2016). Commensal bacteria-induced inflammasome activation in mouse and human macrophages is dependent on potassium efflux but does not require phagocytosis or bacterial viability. *PLOS ONE*, 11(8), Article e0160937. <https://doi.org/10.1371/journal.pone.0160937>

Correa-Costa, M., Braga, T. T., Semedo, P., Hayashida, C. Y., Bechara, L. R., Elias, R. M., & Cunha, F. Q. (2011). Pivotal role of Toll-like receptors 2 and 4, its adaptor molecule MyD88, and inflammasome complex in experimental tubule-interstitial nephritis. *PLOS ONE*, 6(12), Article e29004. <https://doi.org/10.1371/journal.pone.0029004>

Cui, D., Liu, S., Tang, M., Lu, Y., Zhao, M., Mao, R., & Zhang, W. (2020). Phloretin ameliorates hyperuricemia-induced chronic renal dysfunction through inhibiting NLRP3 inflammasome and uric acid reabsorption. *Phytomedicine*, 66, 153111. <https://doi.org/10.1016/j.phymed.2019.153111>

De la Fuente, M., Franchi, L., Araya, D., Díaz-Jiménez, D., Olivares, M., Álvarez-Lobos, M., & Sánchez, A. (2014). Escherichia coli isolates from inflammatory bowel diseases patients survive in macrophages and activate NLRP3 inflammasome. *International Journal of Medical Microbiology*, 304(3–4), 384–392. <https://doi.org/10.1016/j.ijmm.2014.02.003>

Elinav, E., Thaiss, C. A., & Flavell, R. A. (2013). Analysis of microbiota alterations in inflammasome-deficient mice. *Methods in Molecular Biology*, 1040, 185–194. https://doi.org/10.1007/978-1-62703-617-8_12

Feng, Y., Shi, T., Fu, Y., & Lv, B. (2022). Traditional Chinese medicine to prevent and treat diabetic erectile dysfunction. *Frontiers in Pharmacology*, 13, 956173. <https://doi.org/10.3389/fphar.2022.956173>

Ge, P., Chang, Q., Wu, Q., & Guo, Y. (2018). Effect of Quyu Huatan Erxian Decoction combined with febuxostat on vascular endothelial function and erectile dysfunction in patients with hyperuricemia. *Guangdong Medical Journal*, 39(21), 3270–3272. <https://doi.org/10.3969/j.issn.1001-9448.2018.21.027>

Ge, P., & Guo, Y. (2020). Effect of Quyu Huatan Erxian Decoction combined with febuxostat on penile

- hemodynamics and erectile dysfunction in patients with hyperuricemia. *Practical Clinical Journal of Integrated Traditional Chinese and Western Medicine*, 20(14), 1–38.
- Hirota, S. A., Ng, J., Lueng, A., Khajah, M., Parhar, K., Li, Y., & McManus, B. M. (2011). NLRP3 inflammasome plays a key role in the regulation of intestinal homeostasis. *Inflammatory Bowel Diseases*, 17(6), 1359–1372. <https://doi.org/10.1002/ibd.21480>
- Hou, Y., Luo, D., Hou, Y., Luan, J., Zhan, J., Chen, Z., & Wu, Y. (2022). Bu Shen Huo Xue decoction promotes functional recovery in spinal cord injury mice by improving the microenvironment to promote axonal regeneration. *Chinese Medicine*, 17(1), 85. <https://doi.org/10.1186/s13020-022-00484-w>
- Huang, Y., Jiang, H., Chen, Y., Wang, X., Yang, Y., Tao, J., & Li, J. (2018). Tranilast directly targets NLRP3 to treat inflammasome-driven diseases. *EMBO Molecular Medicine*, 10(4), Article e8689. <https://doi.org/10.15252/emmm.201708689>
- Ibrahim, A., Ali, M., Kiernan, T. J., & Stack, A. G. (2018). Erectile dysfunction and ischaemic heart disease. *European Cardiology*, 13(2), 98–103. <https://doi.org/10.15420/ecr.2018.13.2.98>
- Ising, C., Venegas, C., Zhang, S., Scheiblich, H., Schmidt, S. V., Vieira-Saecker, A., & Heneka, M. T. (2019). NLRP3 inflammasome activation drives tau pathology. *Nature*, 575(7784), 669–673. <https://doi.org/10.1038/s41586-019-1721-3>
- Jin, M., Yang, F., Yang, I., Yin, Y., Luo, J. J., Wang, H., & Tang, M. (2012). Uric acid, hyperuricemia, and vascular diseases. *Frontiers in Bioscience*, 17(2), 656–669. <https://doi.org/10.2741/3987>
- Kato, M., Hisatome, I., Tomikura, Y., Kotani, K., Kinugawa, T., Ogino, K., & Nakamura, T. (2005). Status of endothelial dependent vasodilation in patients with hyperuricemia. *American Journal of Cardiology*, 96(11), 1576–1578. <https://doi.org/10.1016/j.amjcard.2005.07.058>
- Kolasa, T., Matulenko, M. A., Hakeem, A. A., Patel, M. V., Mortell, K., Bhatia, P., & Mehta, P. (2006). 1-Aryl-3-(4-pyridine-2-ylpiperazin-1-yl)propan-1-one oximes as potent dopamine D4 receptor agonists for the treatment of erectile dysfunction. *Journal of Medicinal Chemistry*, 49(17), 5093–5109. <https://doi.org/10.1021/jm0603645>
- Koroglu, G., Kaya-Sezginer, E., Yilmaz-Oral, D., & Gur, S. (2018). Management of erectile dysfunction: An under-recognition of hypertension. *Current Pharmaceutical Design*, 24(30), 3506–3519. <https://doi.org/10.2174/1381612824666180213144543>
- Latz, E., Xiao, T. S., & Stutz, A. (2013). Activation and regulation of the inflammasomes. *Nature Reviews Immunology*, 13(6), 397–411. <https://doi.org/10.1038/nri3468>
- Li, H., Xu, W., Liu, X., Wang, T., Wang, S., Liu, J., & Zhang, H. (2021). JAK2 deficiency improves erectile function in diabetic mice through attenuation of oxidative stress, apoptosis, and fibrosis. *Andrology*, 9(5), 1662–1671. <https://doi.org/10.1111/andr.13013>
- Liu, L., Xu, X., Zhang, N., Zhang, Y., & Zhao, K. (2020). Acetylase inhibitor SI-2 is a potent anti-inflammatory agent by inhibiting NLRP3 inflammasome activation. *International Immunopharmacology*, 87, 106829. <https://doi.org/10.1016/j.intimp.2020.106829>
- Liu, R., Han, C., Wu, D., Xia, X., Gu, J., Guan, H., & Zhang, Y. (2015). Prevalence of hyperuricemia and gout in mainland China from 2000 to 2014: A systematic review and meta-analysis. *Biomedical Research International*, 2015, 762820. <https://doi.org/10.1155/2015/762820>
- Liu, W. C., Hung, C. C., Chen, S. C., Yeh, S. M., Lin, M. Y., Chiu, Y. W., & Hsu, C. Y. (2012). Association of hyperuricemia with renal outcomes, cardiovascular disease, and mortality. *Clinical Journal of the American Society of Nephrology*, 7(4), 541–548. <https://doi.org/10.2215/CJN.08360811>
- Long, H., Jiang, J., Xia, J., Jiang, R., He, Y., Lin, H., & Li, X. (2016). Hyperuricemia is an independent risk factor for erectile dysfunction. *Journal of Sexual Medicine*, 13(7), 1056–1062. <https://doi.org/10.1016/j.jsxm.2016.05.015>
- Lv, Z., Lv, D. Y., Meng, J. Y., Sha, X. Y., Qian, X. Y., Chen, Y. S., & Zhang, L. (2023). Trophoblastic mitochondrial DNA induces endothelial dysfunction and NLRP3 inflammasome activation: Implications for preeclampsia. *International Immunopharmacology*, 114, 109523. <https://doi.org/10.1016/j.intimp.2023.109523>
- Martinon, F., Pétrilli, V., Mayor, A., Tardivel, A., & Tschopp, J. (2006). Gout-associated uric acid crystals activate the NALP3 inflammasome. *Nature*, 440(7081), 237–241. <https://doi.org/10.1038/nature04516>
- Mulay, S. R., Kulkarni, O. P., Rupanagudi, K. V., Migliorini, A., Darisipudi, M. N., Vilaysane, A., & Anders, H. J. (2013). Calcium oxalate crystals induce renal inflammation by NLRP3-mediated IL-1 β secretion. *Journal of Clinical Investigation*, 123(1), 236–246. <https://doi.org/10.1172/JCI65489>
- Nagahama, K., Iseki, K., Inoue, T., Touma, T., Ikemiya, Y., & Takishita, S. (2004). Hyperuricemia and cardiovascular risk factor clustering in a screened cohort in Okinawa, Japan. *Hypertension Research*, 27(4), 227–233. <https://doi.org/10.1291/hypres.27.227>
- Pan, D., Xu, Z. H., Gao, Q., Li, M., Guan, Y., & Zhao, S. T. (2020). Relationship between penile erection and the ratio of estradiol to testosterone: A retrospective study. *Andrologia*, 52(9), Article e13701. <https://doi.org/10.1111/and.13701>
- Rajasekaran, M., White, S., Baquir, A., & Wilkes, N. (2005). Rho-kinase inhibition improves erectile function in aging male Brown-Norway rats. *Journal of Andrology*, 26(2), 182–188. <https://doi.org/10.1002/j.1939-4640.2005.tb00052.x>
- Roumeguère, T., Sternon, J., & Schulman, C. C. (2003). Erectile dysfunction and phosphodiesterase type 5 inhibitors. *Revue Médicale de Bruxelles*, 24(3), 169–175.
- Seo, S. U., Kamada, N., Muñoz-Planillo, R., Kim, Y. G., Kim, D., Koizumi, Y., & Nunez, G. (2015). Distinct commensals induce interleukin-1 β via NLRP3 inflammasome in inflammatory monocytes to promote intestinal

- inflammation in response to injury. *Immunity*, 42(4), 744–755. <https://doi.org/10.1016/j.immuni.2015.03.013>
- Shamloul, R., & Ghanem, H. (2013). Erectile dysfunction. *The Lancet*, 381(9861), 153–165. [https://doi.org/10.1016/S0140-6736\(12\)60520-0](https://doi.org/10.1016/S0140-6736(12)60520-0)
- Sobrano Fais, R., Menezes da Costa, R., Carvalho Mendes, A., Mestriner, F., Comerma-Steffensen, S. G., Tostes, R. C., & Cava, M. A. (2023). NLRP3 activation contributes to endothelin-1-induced erectile dysfunction. *Journal of Cellular and Molecular Medicine*, 27(1), 1–14. <https://doi.org/10.1111/jcmm.17268>
- Sun, Z. R., Liu, H. R., Hu, D., Fan, M. S., Wang, M. Y., An, M. F., & Chen, S. (2021). Ellagic acid exerts beneficial effects on hyperuricemia by inhibiting xanthine oxidase and NLRP3 inflammasome activation. *Journal of Agricultural and Food Chemistry*, 69(43), 12741–12752. <https://doi.org/10.1021/acs.jafc.1c04985>
- Vilaysane, A., Chun, J., Seamone, M. E., Wang, W., Chin, R., Hirota, S., & McManus, B. M. (2010). The NLRP3 inflammasome promotes renal inflammation and contributes to chronic kidney disease. *Journal of the American Society of Nephrology*, 21(10), 1732–1744. <https://doi.org/10.1681/ASN.2010030313>
- Wang, Y., Lou, X. T., Shi, Y. H., Tong, Q., & Zheng, G. Q. (2019). Erxian decoction, a Chinese herbal formula, for menopausal syndrome: An updated systematic review. *Journal of Ethnopharmacology*, 234, 8–20. <https://doi.org/10.1016/j.jep.2019.01.027>
- Wen, L., Yang, H., Ma, L., & Fu, P. (2021). The roles of NLRP3 inflammasome-mediated signaling pathways in hyperuricemic nephropathy. *Molecular and Cellular Biochemistry*, 476(3), 1377–1386. <https://doi.org/10.1007/s11010-021-04194-2>
- Wu, Q., Liu, M. C., Yang, J., Wang, J. F., & Zhu, Y. H. (2016). Lactobacillus rhamnosus GR-1 ameliorates Escherichia coli-induced inflammation and cell damage via attenuation of ASC-independent NLRP3 inflammasome activation. *Applied and Environmental Microbiology*, 82(4), 1173–1182. <https://doi.org/10.1128/AEM.03416-15>
- Wu, H., Gao, Z., Dai, D., Liu, X., Fang, Y., Chen, X., & Wang, Q. (2023). Efficacy and safety assessment of traditional Chinese medicine for erectile dysfunction: A meta-analysis and trial sequential analysis. *Andrology*, 11(7), 1345–1367. <https://doi.org/10.1111/andr.13273>
- Xiao, L., Li, X., Cao, P., Fei, W., Zhou, H., Tang, N., & Zhang, Z. (2022). Interleukin-6 mediated inflammasome activation promotes oral squamous cell carcinoma progression via JAK2/STAT3/Sox4/NLRP3 signaling pathway. *Journal of Experimental & Clinical Cancer Research*, 41(1), 166. <https://doi.org/10.1186/s13046-022-02260-x>
- Xie, H., Jin, H., Chen, L., Chen, Z., Ge, P., & Yang, M. (2023). Effect of Quyu Huatan Erxian Decoction on inflammatory corpuscles of corpus cavernosum NLRP3 in aged rats with hyperuricemia. *Practical Clinical Journal of Integrated Traditional Chinese and Western Medicine*, 23(3), 1–5.
- Xing, J. H., Li, R., Gao, Y. Q., Wang, M. Y., Liu, Y. Z., Hong, J., & Zhang, H. (2019). NLRP3 inflammasome mediates palmitate-induced endothelial dysfunction. *Life Sciences*, 239, 116882. <https://doi.org/10.1016/j.lfs.2019.116882>
- Xu, Z., Xie, W., Feng, Y., Wang, Y., Li, X., Liu, J., & Zhang, Y. (2022). Positive interaction between GPER and β -alanine in the dorsal root ganglion uncovers potential mechanisms: Mediating continuous neuronal sensitization and neuroinflammation responses in neuropathic pain. *Journal of Neuroinflammation*, 19(1), 164. <https://doi.org/10.1186/s12974-022-02649-3>
- Yavuzgil, O., Altay, B., Zoghi, M., Gürgün, C., Kayıkçioğlu, M., & Kültürsay, H. (2005). Endothelial function in patients with vasculogenic erectile dysfunction. *International Journal of Cardiology*, 103(1), 19–26. <https://doi.org/10.1016/j.ijcard.2004.07.039>
- Zhang, Y., Wang, S., Dai, X., Liu, T., Liu, Y., Shi, H., & Xie, L. (2023). Simiao San alleviates hyperuricemia and kidney inflammation by inhibiting NLRP3 inflammasome and JAK2/STAT3 signaling in hyperuricemia mice. *Journal of Ethnopharmacology*, 312, 116530. <https://doi.org/10.1016/j.jep.2023.116530>
- Zhu, Y., Pandya, B. J., & Choi, H. K. (2011). Prevalence of gout and hyperuricemia in the US general population: The National Health and Nutrition Examination Survey 2007–2008. *Arthritis & Rheumatism*, 63(10), 3136–3141. <https://doi.org/10.1002/art.30520>